https://doi.org/10.1016/j.apacoust.2017.02.006
This is the Pre-Published Version.

Technical Note

Noise attenuation performance improvement by adding Helmholtz resonators on the periodic ducted Helmholtz resonator system

Chenzhi Cai [a], Cheuk Ming Mak [a, *] and Xu Wang [b]

[a] *Department of Building Services Engineering, The Hong Kong Polytechnic University, Hung Hom, Kowloon, Hong Kong, China*

[b] *Institute of Acoustics, Tongji University, No. 1239 Siping Road, Shanghai 200092, China*

chenzhi.cai@connect.polyu.hk, cheuk-ming.mak@polyu.edu.hk

*Corresponding author.
E-mail Address: cheuk-ming.mak@polyu.edu.hk (C.M.Mak).
Telephone: +852 2766 5856
Fax: +852 2765 7198

© 2017. This manuscript version is made available under the CC-BY-NC-ND 4.0 license https://creativecommons.org/licenses/by-nc-nd/4.0/

Abstract

This paper focuses on improving the noise attenuation performance of a ducted Helmholtz resonator (HR) system and fully utilizing an available space. The transmission loss achieved by a periodic ducted HR system is depended on the structure and the number of HRs. However, the number of HRs is restricted by the available space in longitudinal direction of the duct. Moreover, such system will occupy a large space and may have some spare space in the transverse direction of the duct. By adding HRs on the available space in the transverse direction, a modified ducted HR system is therefore proposed. The wave propagation in the periodic ducted HR system and the modified HR system are investigated theoretically and numerically. The transfer matrix method is developed to conduct the investigation. The predicted theoretical results fit well with the Finite Element Method (FEM) simulation results. The results indicate that both the noise attenuation band and peak amplitude are increased by adding HRs on arbitrary side of the cross-section of the duct. The proposed modified ducted HR system can improve the noise attenuation performance and fully utilize the available space, and it is practical to be used in an actual ventilation ductwork system.

Keywords: Helmholtz resonator; space utilization; noise control; transmission loss

1. Introduction

Ventilation ductwork system is essential constituent part in many engineering applications, especially in modern buildings that maintains good indoor air quality. However, as the ventilation ductwork system begins to operate, the in-ducted elements such as dampers, sensors, bends transition pieces, duct corners, branch points or even attenuators can generate undesired noise [1]. The accompanied noise can be a disturbance to human activities. It is therefore important to reduce duct-borne noise, especially the low-frequency and broadband noise in the ventilation ductwork system [2,3]. One traditional passive method for noise control at mid frequencies is the use of dissipative silencer in which the sound absorption materials in the silencers dissipate the sound energy into heat [4]. However, the acoustical properties and the damping mechanism of the sound absorption materials determine that it is not effective for low-frequency noise control. An active noise control system can provide environmental-adaptive noise attenuation and there have been efforts attempting to active noise control application in recent years. Although the active noise control has been successfully implemented in practical application and has great potential advantage of controlling low frequencies noise, the reliability and high cost are important challenges for engineering [5,6]. Passive reactive silencer, the Helmholtz resonator (hereafter HR), that qualifies as a narrow band noise attenuator, is commonly used to reduce low-frequency noise at its resonance peak [7,8]. The resonance frequency of a HR is only determined by the geometries of the cavity and the neck. It is therefore easy to design a HR with a desired resonance frequency.

Since a single HR has a narrow noise attenuation band, an array of HRs is one way to obtain a broader noise attenuation band. Many researchers and engineers around the world have devoted their attention to broaden the noise attenuation band. A lot of achievements have been made and are documented in numerous pieces of literature. Seo and Kim [9] aimed to broaden the narrow band characteristics by combing many resonators and optimized the arrangement of resonators. Sugimoto and Horioka [10] presented the peculiar dispersion characteristics of sound waves propagation in a tunnel with periodic ducted HRs, marked as stopbands and passbands. Wang and Mak [11] examined the disorder in the geometries of HRs and the disorder in periodic distance to achieve a relatively wide noise attenuation band. Chiu [12] studied the hybrid HR mufflers to deal with a broadband noise hybridized with a pure tone and presented the numerical assessment to evaluate the acoustic performance of a multi-tone hybrid Helmholtz muffler. Coulon et al. [13] investigated the role of distance between HRs on the transmission loss of the whole HR array system and proposed an optimization approach for wide band noise attenuation.

This paper focuses on improving the noise attenuation performance of a ducted HR system and fully utilizing the available space. The transmission loss achieved by a periodic ducted HR system is depended on the structure and the number of HRs. Owing to the coupling of Bragg reflection and HR’s resonance, it is found that a periodic ducted HR system can provide much broader noise attenuation band. However, the noise attenuation performance of the system fairly depends on the number of HRs. The number of HRs is restricted by the available space in longitudinal direction of the duct and many HRs are needed in order to obtain the required noise attenuation band. Such system will occupy a large space and may have some spare space in transverse direction of the duct. By adding

HRs on the available space in the transverse direction, a modified ducted HR system is therefore proposed in this paper. As low frequencies are more important in ventilation noise control, the frequency range considered in this paper is well below the duct's cutoff frequency. For this reason, only planar wave is assumed to propagate through the duct. The transfer matrix is therefore developed to investigate the acoustic performance of the ducted HR system. The proposed model is validated by Finite Element Method (FEM) simulation. The proposed modified ducted HR system is practical to be used in an actual ventilation ductwork system to improve the noise attenuation performance of the ducted HR system and to fully utilize the available space.

2. Theoretical analysis of side-branch Helmholtz resonators

2.1 Transmission loss of a single side-branch HR

The Helmholtz resonator, which consists of a cavity communicating with an external duct through a neck, is traditionally considered as an equivalent mass-spring model with end-correction factors for the sake of the accuracy. The mass of air in the neck is driven by an external force and the cavity is regarded as the spring [14]. Furthermore, wave propagation in both the duct and the HR has been considered in theoretical analysis. The wave propagation approach developed from a one-dimensional approach in preliminary investigations to a multidimensional approach in order to account for nonplanar effects, and the latter has been proven by experiment to be a better theoretical analysis approach [15,16]. Although a multidimensional approach provides a more accurate measure of the acoustic impedance of the HR, the main purpose here is to reveal the acoustic performance of the proposed modified ducted HR system. For this reason, the classical model is adopted here and the acoustic impedance of the HR is given as [7]:

$$Z_r = j\frac{\rho_0 l_n'}{S_n \omega}(\omega^2 - \omega_0^2) \tag{1}$$

where ρ_0 is air density, l_n' and S_n are the neck's effective length and area respectively, $\omega_0 = c_0\sqrt{S_n / l_n' V_c}$ (V_c is the cavity volume and c_0 is the speed of sound in the air) and ω are the resonant circular frequency and circular frequency respectively.

A single side-branch HR is shown in Fig.1. On the basis of low-frequency range considered in this paper, only planar wave is assumed to propagate in the duct. By ignoring the time-harmonic disturbance and the reflected waves from downstream of the duct, the sound pressure and particle velocity can be expressed as:

$$p_1(x) = I_1 e^{-jkx} + R_1 e^{jkx},\ \ p_2(x) = I_2 e^{-jkx} \tag{2}$$

$$u_1(x) = \frac{I_1}{S_d Z_d} e^{-jkx} - \frac{R_1}{S_d Z_d} e^{jkx},\ \ u_2(x) = \frac{I_2}{S_d Z_d} e^{-jkx} \tag{3}$$

where k is the wave number, S_d is the cross-sectional area of the duct, Z_d is the acoustic impedance of the duct, and I_i (i=1,2) and R_1 represent respective complex wave amplitudes. Combining the continuity of sound pressure and volume velocity at the duct-neck interface at $x = 0$ yields:

$$\begin{bmatrix} p_1 \\ \rho_0 c_0 u_1 \end{bmatrix} = \begin{pmatrix} 1 & 0 \\ \frac{\rho_0 c_0}{S_d}\frac{1}{Z_r} & 1 \end{pmatrix} \begin{bmatrix} p_2 \\ \rho_0 c_0 u_2 \end{bmatrix} \tag{4}$$

Then the transmission loss of a single side-branch HR can be determined by the four-pole parameters method [17] as:

$$TL = 20\log_{10}\left(\frac{1}{2}\left| 2 + \frac{\rho_0 c_0}{S_d}\frac{1}{Z_r} \right|\right) \tag{5}$$

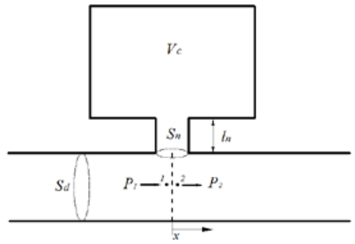

Fig. 1 A single side-branch Helmholtz resonator.

2.2 Transmission loss of the side-branch HRs

It is well known that a single HR has a high transmission loss peak with narrow band. Several identical HRs installed on the same cross-section of the duct is a possible way to broaden the noise attenuation band [9,12]. The side-branch HRs with N (N=4 here for example) identical HRs mounted on the same cross-section of the duct is illustrated in Fig. 2.

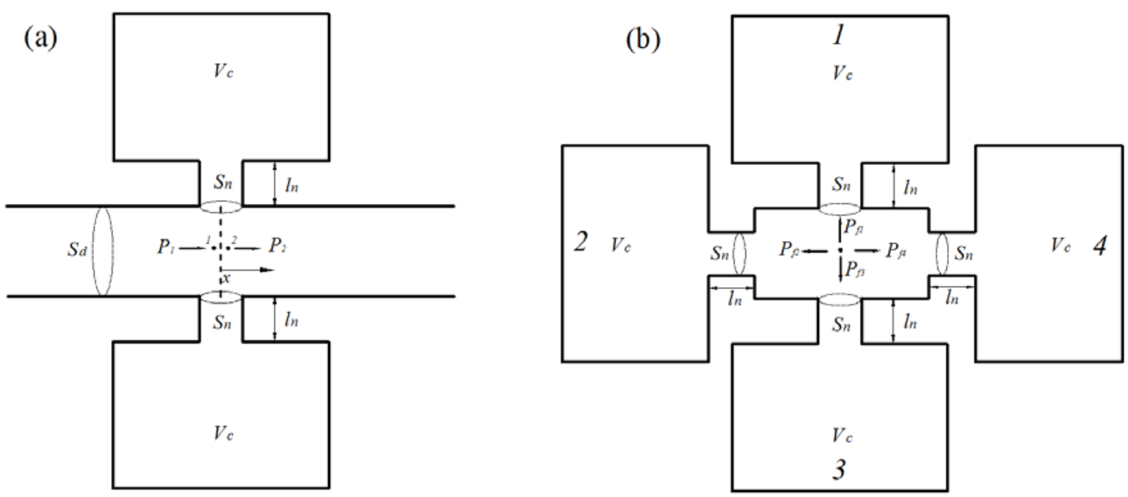

Fig. 2 A side-branch Helmholtz resonators (a) side view (b) front view.

Similarly, by ignoring the time-harmonic disturbance and the reflected waves from downstream of the duct, the sound pressure and particle velocity of point 1 and point 2, as shown in Fig. 2 (a), can be expressed by Eq. (2) and Eq. (3) respectively. As depicted in Fig. 2 (b), the continuity condition of sound pressure at the duct-neck interface gives:

$p_1 = p_2 = p_{fi}$ (i=1,2,3,4 represents each individual HR). The continuity condition of volume velocity at the same interface gives: $S_d u_1 = S_d u_2 + \sum_i^N p_{fi} / Z_r$. The relation of point 1 to point 2 could be obtained by combining the continuity condition above. Then, according to the four-pole parameter method, the transmission loss of the side-branch HRs can be expressed as:

$$TL = 20\log_{10}\left(\frac{1}{2}\left|2 + N\frac{\rho_0 c_0}{S_d}\frac{1}{Z_r}\right|\right) \tag{6}$$

According to Eq. (6), it can be seen that the resonance frequency of side-branch HRs system still depends on the single HR. Several identical HRs mounted on the same cross-section of the duct could be considered as an equivalent “one HR” with acoustic impedance of Z_r / N . It indicates that the equivalent “one HR” remains the same resonance frequency as the single HR. The added HRs improve both the peak amplitudes and the attenuation band. It inspires us to improve the acoustic performance of the periodic ducted HRs system by adding HRs on the transverse direction of the duct.

3. Theoretical analysis of ducted Helmholtz resonators systems

3.1 Transmission loss of the periodic ducted HR system

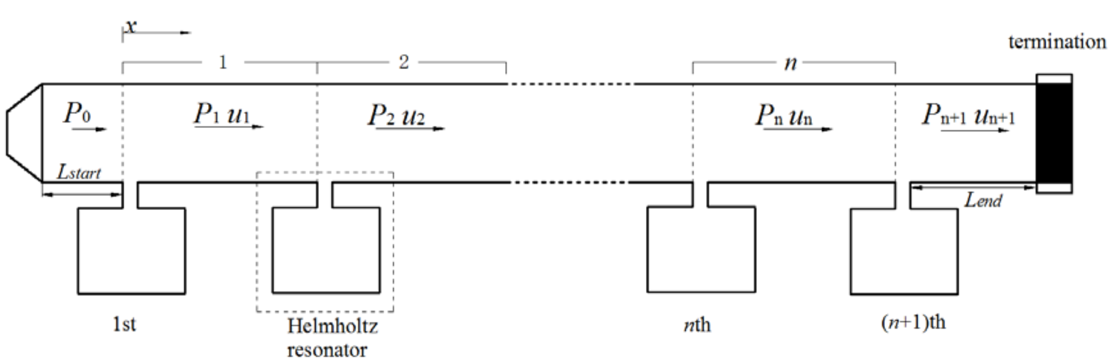

Fig. 3 Schematic diagram of a periodic ducted HR system.

An array of lined HRs mounted periodically on the duct, as shown in Fig. 3, is investigated firstly. A duct segment with a HR constitutes a typical periodic cell. By assuming the diameter of the HR's neck is negligible compared with the length of duct segment in a periodic cell, it is therefore that the duct segment's length is regarded as the periodic distance. In the nth cell, the sound properties can be described as sound pressure $p_n(x)$ and particle velocity $u_n(x)$. The frequency range considered in this paper is well below the cutoff frequency of the duct. The sound pressure is a combination of positive-*x* and negative-*x* directions. Assuming a time-harmonic disturbance in the form of $e^{j\omega t}$, the sound pressure and particle velocity are expressed as:

$$p_n(x) = I_n e^{-jk(x-x_n-\omega t)} + R_n e^{jk(x-x_n+\omega t)} \tag{7}$$

$$u_n(x) = \frac{I_n}{S_d Z_d} e^{-jk(x-x_n-\omega t)} - \frac{R_n}{S_d Z_d} e^{jk(x-x_n+\omega t)} \tag{8}$$

where k is the number of waves, $x_n = (n-1)d$ represents the local coordinates, d is the periodic distance, S_d is the cross-sectional area of the duct, Z_d is the acoustic impedance of the duct, and I_n and R_n represent respective complex wave amplitudes. Combining the continuity of sound pressure and volume velocity at $x = nd$ yields:

$$\begin{bmatrix} I_{n+1} \\ R_{n+1} \end{bmatrix} = \begin{bmatrix} (1-\frac{Z_d}{2Z_r})\exp(-jkd) & -\frac{Z_d}{2Z_r}\exp(jkd) \\ \frac{Z_d}{2Z_r}\exp(-jkd) & (1+\frac{Z_d}{2Z_r})\exp(jkd) \end{bmatrix} \begin{bmatrix} I_n \\ R_n \end{bmatrix} = \mathbf{T} \begin{bmatrix} I_n \\ R_n \end{bmatrix} \tag{9}$$

$\mathbf{T}$ is the transfer matrix. Once the initial sound pressure is given, the sound pressure and particle velocity in an arbitrary cell can be determined successively by Eq. (9). According to Bloch wave theory [18], Eq. (9) can be rewritten as:

$$\begin{bmatrix} I_{n+1} \\ R_{n+1} \end{bmatrix} = \lambda \begin{bmatrix} I_n \\ R_n \end{bmatrix} = \mathbf{T} \begin{bmatrix} I_n \\ R_n \end{bmatrix} \tag{10}$$

where λ is set to be $\exp(-jqd)$, and q is the Bloch wave number and is allowed to be a complex value. The analysis of the periodic structure translates to an eigenvalue and its corresponding eigenvector problem. There are two eigenvalue solutions of λ: λ_1 and λ_2 with corresponding eigenvectors $[v_{I1}, v_{R1}]^{\mathbf{T}}$ and $[v_{I2}, v_{R2}]^{\mathbf{T}}$ respectively. According to the definition of the eigenvalue, Eq. (10) can be expressed in eigenvector form as:

$$\begin{bmatrix} I_{n+1} \\ R_{n+1} \end{bmatrix} = \mathbf{T} \begin{bmatrix} I_n \\ R_n \end{bmatrix} = \mathbf{T}^2 \begin{bmatrix} I_{n-1} \\ R_{n-1} \end{bmatrix} = \ldots = \mathbf{T}^n \begin{bmatrix} I_1 \\ R_1 \end{bmatrix} = A_0 \lambda_1^n \begin{bmatrix} v_{I1} \\ v_{R1} \end{bmatrix} + B_0 \lambda_2^n \begin{bmatrix} v_{I2} \\ v_{R2} \end{bmatrix} \tag{11}$$

where A_0 and B_0 are complex constants determined by boundary conditions. The end boundary conditions with reflection coefficient α give:

$$\frac{R_n e^{jk(x-x_n+\omega t)}}{I_n e^{-jk(x-x_n-\omega t)}} = \frac{A_0 \lambda_1^{n-1} v_{R1} e^{jkL_{end}} + B_0 \lambda_1^{n-1} v_{R2} e^{jkL_{end}}}{A_0 \lambda_1^{n-1} v_{I1} e^{-jkL_{end}} + B_0 \lambda_1^{n-1} v_{I2} e^{-jkL_{end}}} = \alpha \tag{12}$$

Similarly, the initial condition gives:

$$\begin{aligned} p_0 &= I_0 e^{-jk(x+d)} + R_0 e^{jk(x+d)} \Big|_{x=-L_{start}} \\ &= (A_0 \lambda_1^{-1} v_{I1} + B_0 \lambda_2^{-1} v_{I2}) e^{-jk(d-L_{start})} + (A_0 \lambda_1^{-1} v_{R1} + B_0 \lambda_2^{-1} v_{R2}) e^{jk(d-L_{start})} \end{aligned} \tag{13}$$

Thus the average transmission loss of per HR in the whole system can be expressed as:

$$\overline{TL} = \frac{20}{n+1} \log_{10} \left| \frac{I_0}{I_{n+1}} \right| = \frac{20}{n+1} \log_{10} \left| \frac{A_0 \lambda_1^{-1} v_{I1} + B_0 \lambda_2^{-1} v_{I2}}{A_0 \lambda_1^{n-1} v_{I1} + B_0 \lambda_2^{n-1} v_{I2}} \right| \tag{14}$$

When the duct ends with an anechoic termination, the reflection α equals zero, and λ_1 describes positive-direction propagation, it means that $|\lambda_1| < 1, |\lambda_2| > 1$. $B_0 = 0$ is required in this situation. The average transmission loss of a duct with an anechoic termination can be expressed as: $\overline{TL} = -20\log_{10}|\lambda_1|$. The solution of λ is a function of wave frequency, periodic distance and the geometric dimensions of the ducted HR system. Generally, there are two formation mechanisms for the noise attenuation band: the HR's resonance mechanism and the Bragg reflection. Once the periodic distance is chosen to be $d = \lambda_0/2$, the designed HR's resonance frequency coincides with the first Bragg reflection. In this situation, a broader noise attenuation band at resonance frequency could be achieved [10,19].

3.2 Transmission loss of modified ducted HR system

A duct with periodic distributed identical HR has a unique attenuation characteristic due to the coupling of Bragg reflection and HR's resonance. However, for every single HR in the periodic ducted HR system, the noise attenuation capacity remains unchanged in spite of HR's number or the periodic distance. The broader the noise attenuation band, the lower the peak amplitude [20]. It indicates that the transmission loss achievable by periodic ducted HR system is fairly depended on the HR's number, which is restricted to the available space in longitudinal direction of the duct. Besides, for a periodic system, there may also have some spare space in transverse direction of the duct. It is therefore that a modified ducted HR system is proposed to improve the noise attenuation performance and to fully utilize the available space. As illustrated in Fig. 4, HRs are added on the cross-section of the periodic ducted HR system to form the modified ducted HR system. The number of HRs mounted on the same cross-section depends on the available space. Each cell of the modified ducted HR system could comprise different number of HRs. As discussed above, several identical HRs mounted on the same cross-section of the duct could be considered as an equivalent "one HR" with acoustic impedance of Z_r / N.

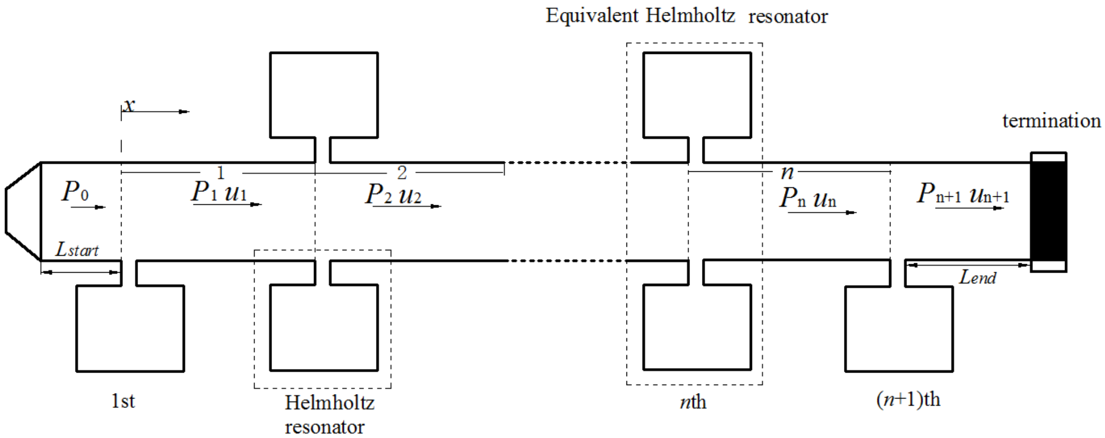

Fig. 4 Schematic diagram of a modified ducted HR system.

It is therefore that the system can no longer be represented by the single transfer matrix $\mathbf{T}$ derived from Eq. (9). Instead, the transfer matrix between each two nearby cell should be specified as $\mathbf{T}_n$. Similar to the periodic ducted HR system, the sound characteristics in *nth* segment could be expressed by Eq. (7) and Eq. (8). By intruding the continuity conditions, the transfer matrix between *nth* and $n+1$*th* segment could be expressed as:

$$\begin{bmatrix} I_{n+1} \\ R_{n+1} \end{bmatrix} = \begin{bmatrix} (1-N\dfrac{Z_d}{2Z_r})\exp(-jkd) & -N\dfrac{Z_d}{2Z_r}\exp(jkd) \\ N\dfrac{Z_d}{2Z_r}\exp(-jkd) & (1+N\dfrac{Z_d}{2Z_r})\exp(jkd) \end{bmatrix} \begin{bmatrix} I_n \\ R_n \end{bmatrix} = \mathbf{T}_n \begin{bmatrix} I_n \\ R_n \end{bmatrix} \tag{15}$$

The complex wave amplitudes can be rewritten into a state vector as $\mathbf{a}_{n+1} = [I_{n+1} \quad R_{n+1}]^T$, where superscript T means transposition. Then, Eq. (15) could be simplified as:

$$\mathbf{a}_{n+1} = \mathbf{T}_n \mathbf{a}_n \tag{16}$$

The transfer matrix $\mathbf{T}_n$ could also be expressed in form of reflection and transmission coefficients, t_n and r_n as [21]:

$$\begin{bmatrix} I_{n+1} \\ R_{n+1} \end{bmatrix} = \begin{bmatrix} e^{-jkL_n} & 0 \\ 0 & e^{jkL_n} \end{bmatrix} \begin{bmatrix} 1/t_n^{*} & -(r_n/t_n)^{*} \\ -(r_n/t_n) & 1/t_n \end{bmatrix} \begin{bmatrix} I_{n+1} \\ R_{n+1} \end{bmatrix} = \mathbf{T}_n \begin{bmatrix} I_n \\ R_n \end{bmatrix} \tag{17}$$

where the superscript * means conjugation. It follows immediately from Eq. (16) that:

$$\mathbf{a}_{n+1}\mathbf{a}_{n+1}^{T\;*} = \mathbf{T}_n(\mathbf{a}_n\mathbf{a}_n^{T*})\mathbf{T}_n^{T*} \tag{18}$$

Eq. (18) is a matrix equation and it can be re-expressed in vector form as:

$$\mathbf{e}_{n+1} = \mathbf{A}_n\mathbf{e}_n \tag{19}$$

Where $\mathbf{e}_{n+1}$ and $\mathbf{e}_n$ can be represented as: $\left[I_nI_n^{\;*} \quad I_nR_n^{\;*} \quad R_nI_n^{\;*} \quad R_nR_n^{\;*}\right]^T$ and $\left[I_{n+1}I_{n+1}^{\;*} \quad I_{n+1}R_{n+1}^{\;*} \quad R_{n+1}I_{n+1}^{\;*} \quad R_{n+1}R_{n+1}^{\;*}\right]^T$ respectively. According to the Eq. (18) and Eq. (19), the matrix $\mathbf{A}_n$ takes the form of $\mathbf{T}_n$ as [22]:

$$\mathbf{A}_n = \begin{bmatrix} 1/|t_n|^2 & -r_n/|t_n|^2 & -r_n^*/|t_n|^2 & |r_n|^2/|t_n|^2 \\ -r_n^*\delta_n/t_n^{*2} & \delta_n/t_n^{*2} & r_n^{*2}\delta_n/t_n^{*2} & -r_n^*\delta_n/t_n^{*2} \\ -r_n/\delta_n t_n^2 & r_n^2/\delta_n t_n^2 & 1/\delta_n t_n^2 & -r_n/\delta_n t_n^2 \\ |r_n|^2/|t_n|^2 & -r_n/|t_n|^2 & -r_n^*/|t_n|^2 & 1/|t_n|^2 \end{bmatrix} \tag{20}$$

Where $\delta_n = \exp(-2jkd)$ (d should be replaced by L_{start} and L_{end} when sound propagates in the start and end segment of the whole system). It can be seen from Eq. (20) that the value of $\mathbf{A}_n(4,4)$ is $1/|t_n|^2$. It indicates that the transmission loss between these two segments could be described as: $TL = 10\log_{10}(\mathbf{A}_n(4,4))$. When the duct ends with an anechoic termination, the whole HR system can be described as:

$$\mathbf{a}_{n+1} = \mathbf{T}_n\mathbf{a}_n = \mathbf{T}_n\mathbf{T}_{n-1}\mathbf{a}_{n-1} = \cdots = (\prod_{i=0}^{n}\mathbf{T}_i)\mathbf{a}_0 \tag{21}$$

With the introduction of Eq. (18) and Eq. (19), Eq. (21) could be expressed as:

$$\mathbf{e}_{n+1} = \left(\prod_{i=0}^{n}\mathbf{A}_n\right)\mathbf{e}_0 = \Lambda\mathbf{e}_0 \tag{22}$$

where Λ is the matrix of the whole ducted resonator system. Similar to Eq. (20), $\Lambda(4,4)$ equals to the modulus squared transmission coefficient of the whole system. It is therefore that the average transmission loss of per HR in the whole system could be expressed as:

$$\overline{TL} = \frac{10}{N_{total}} \log_{10}\left(\Lambda(4,4)\right) \tag{23}$$

where N_{total} is the sum of HRs mounted on the duct.

4. Results and discussion

4.1 Validation of the predicted transmission loss of side-branch HRs

The single side-branch HR and the side-branch HRs are illustrated in Fig. 1 and Fig. 2 respectively. The geometries of the HR used in this paper are: cavity volume $V_c = 19.4\pi cm^3$, neck area $S_n = 0.25\pi cm^2$ and neck length $l_n = 2.5cm$. The cross-section area of the main duct is $S_d = 25cm^2$. The comparison of the transmission loss (TL) with respect to the number of identical HRs installed on the same cross-section of the duct is shown in Fig. 5. The TL of a side-branch HR has a peak amplitude with narrow attenuation band, as is well known and depicted in Fig. 5 (N=1). By adding identical HRs on the same cross-section of the duct, it can be seen that both the magnitude of TL and the noise attenuation bandwidth are increased obviously. Furthermore, the added HRs has no effect on resonance frequency. The equivalent "one HR" has the same resonance frequency as the single HR.

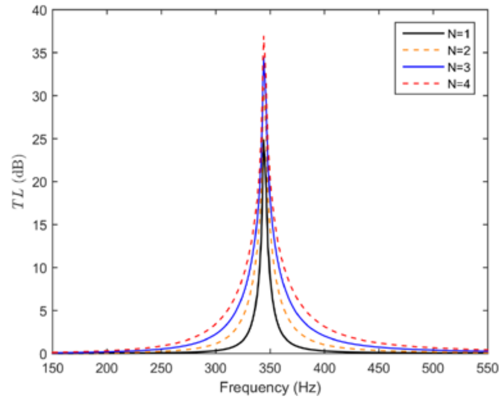

Fig. 5 Comparison of the transmission loss with respect to the number of identical HRs mounted on a same cross-section.

The comparison of the analytical predictions and the FEM simulation with respect to different numbers of HR mounted on the same cross-section is exhibited in Fig. 6. It is shown that the predicted results fit well with the FEM simulation results.

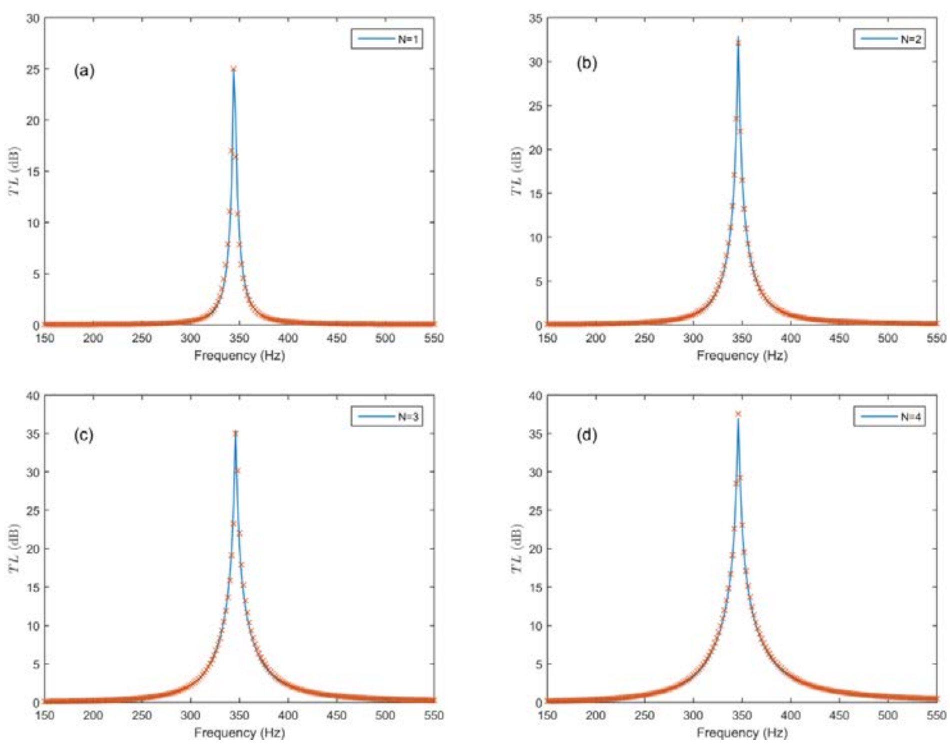

Fig.6 Comparison of the analytical predictions and the FEM simulation with respect to different numbers of HR mounted on the same cross-section (solid lines represents the theoretical predictions, and dotted crosses represent the FEM simulation results).

4.2 Validation of the predicted transmission loss of periodic ducted HR system

The geometries of the HR and the main duct used here is the same as given above. The periodic ducted HR system with an anechoic termination set at the end to avoid reflected waves is shown in Fig. 3. An oscillating sound pressure at a magnitude of $P_0 = 1$ is applied at the beginning of the duct. The periodic distance $d = \lambda_0/2$ is chosen here in order to obtain an broader noise attenuation band. The predicted average transmission loss ($\overline{TL}$) of a periodic ducted HR system with different HR numbers (n=1,4,5,10) are exhibited in Fig. 7.

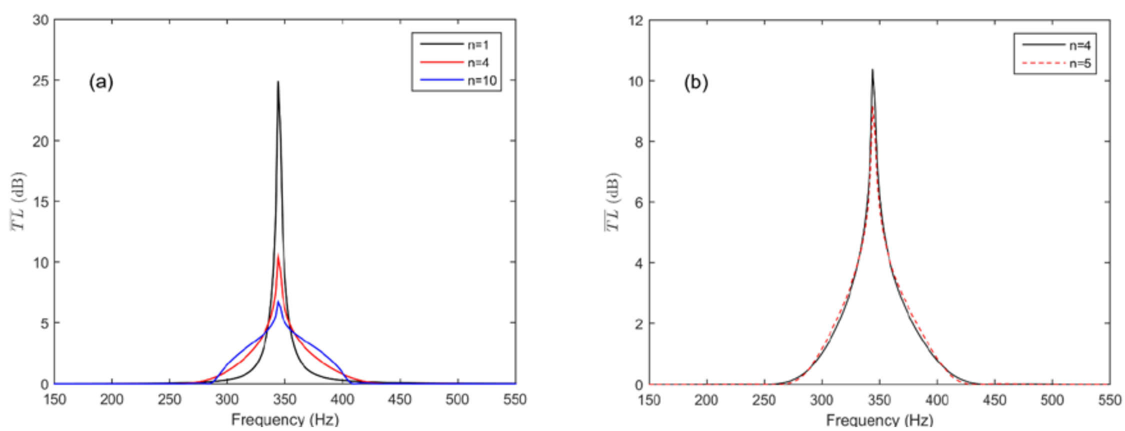

Fig. 7 The average transmission loss of the ducted HR system with different numbers of HR.

The noise attenuation band at the resonance frequency is the combination effect of HR's resonance and Bragg reflection. It can be seen in Fig. 7(a) that with the increase in HRs' number, the peak amplitude decreased with broader attenuation band. However, one more HR added in the periodic system nearly has no effect on $\overline{TL}$, as shown in Fig. 7(b). It indicates that the $\overline{TL}$ changes gradually and its noise attenuation bandwidth is rather related to number of HRs. The comparison of the analytical predictions and the FEM simulation results are illustrated in Fig. 8, and the prediction results are in good agreement with the FEM simulation results.

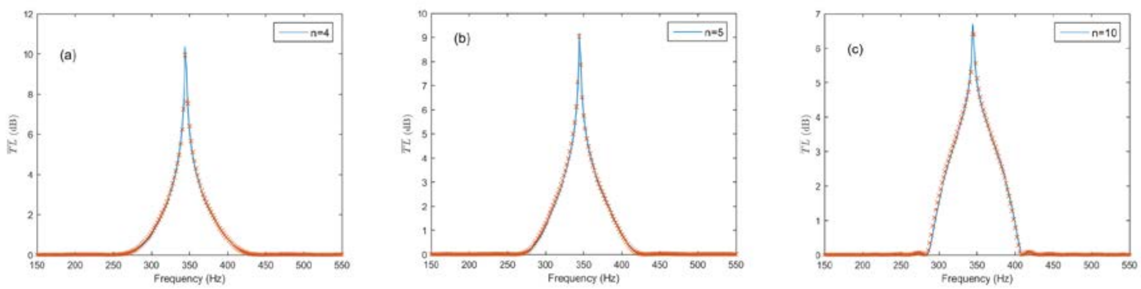

Fig.8 The average transmission loss of the periodic ducted HR system with different number of HRs (solid lines represents the theoretical predictions, and dotted crosses represent the FEM simulation results).

4.3 Validation of the transmission loss of the modified ducted HR system

For a periodic ducted HR system, a broader noise attenuation band could be achieved due to the coupling of the Bragg reflection and HR's resonance. However, such kinds of noise attenuation system will occupy a large space and it is impractical to be used in an actual ventilation ductwork system. The modified ducted HR system, as illustrated in Fig. 4, is proposed to improve the noise attenuation performance and to fully utilize the available space. The geometries of the HR and the main duct are the same as the periodic ducted HR system as given above, as are as the beginning and end conditions. The duct segment length of the modified HR system is set to be $d = \lambda_0/2$ as well. On the basis of low-frequency range considered in this paper, only planar wave is assumed to propagated in the duct. It is therefore that the added HRs can be mounted on arbitrary side of the cross-section of the duct. Fig. 9 shows the configuration of three modified ducted HR system cases: 2143 model ,2131 model and 1121 model respectively.

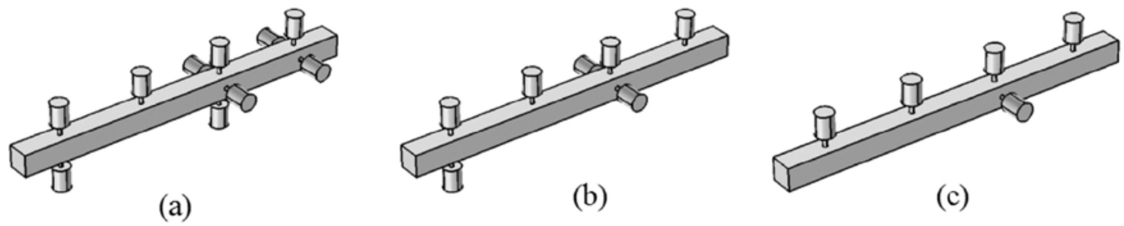

Fig. 9 Configuration of three modified ducted HR system cases: (a) 2143 model, (b) 2131 model, (c) 1121 model (the integer means the number of HR mounted on the same cross-section in consecutive duct segment respectively).

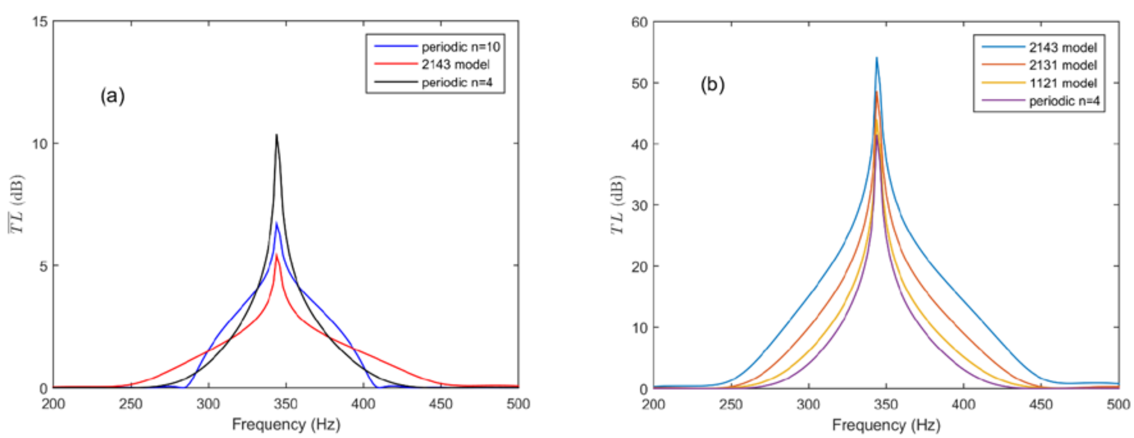

Fig. 10 Comparison of transmission loss with respect to different ducted HR systems: (a) the average transmission loss of per HR in different systems, (b) the total transmission loss of different systems.

Fig. 10(a) compares the $\overline{TL}$ of 2143 model to two periodic ducted HR system cases (*n=4, 10*). The total HR number N_{total} of 2143 model equals to the periodic ducted HR system case *n=10*, while the duct's length of 2143 model is much less than the periodic one. The duct's length of 2143 model is the same as the periodic case *n=4*. However, it can be seen that a broader noise attenuation band could be achieved by this modified ducted HR system.

Furthermore, the 2143 model has broader noise attenuation band and higher peak amplitude than the periodic ducted HR system (case: *n=4*), as shown in Fig. 10(b). The transmission loss of the four different HR systems with same duct segment number is also compared in Fig. 10(b). The comparison shows that both the peak amplitude and noise attenuation band are increased by adding HR on the duct, especially the noise attenuation band. The added HR mounted on the cross-section of the duct mainly broadens the noise attenuation band of the total transmission loss. Moreover, the $\overline{TL}$ bandwidth has an apparent increase due to the added HRs, as shown in Fig. 10(a). A good agreement between the theoretical predicted $\overline{TL}$ and the FEM simulation results can also be seen in Fig. 11. The proposed modified ducted system can improve the noise attenuation performance and fully utilize the available space by adding HRs on arbitrary side of the cross-section of the duct.

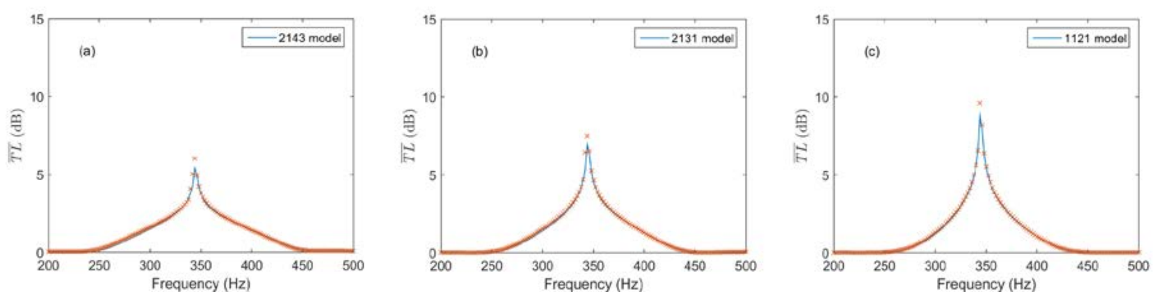

Fig.11 The average transmission loss of different modified HR systems (solid lines represents the theoretical predictions, and dotted crosses represent the FEM simulation results).

5. Conclusion

The transmission loss achieved by a periodic ducted HR system is depended on the structure and the number of HRs. The periodic ducted HR system could provide broader noise attenuation band due to the coupling of the Bragg reflection and the HR's resonance. For the sake of a broader noise attenuation band at the resonance frequency, $d = \lambda_0/2$ is often chosen as a periodic distance. However, the noise attenuation performance of the system fairly depends on the number of HRs, which is restricted by the available space in longitudinal direction of the duct. However, there may have some spare space in the transverse direction of the duct. By adding HRs on the available space in the transverse direction, a modified ducted HR system is proposed. Several identical HRs mounted on a same cross-section of a duct has broader noise attenuation band and higher peak amplitude without effects on the HR's resonance frequency. It means the modified ducted HR can also take full advantage of periodicity to obtain a broader noise attenuation band. Besides, added HRs can improve the noise attenuation performance of the whole system. The more HRs added, the better noise attenuation performance of the system. Moreover, the installation side of the cross-section of the duct for added HRs is arbitrary because only planar wave is assumed to propagate in the duct. It is flexible to install added HRs on the unoccupied space of the transverse direction of the duct. The proposed modified ducted HR system fully utilizes the available space to improve noise attenuation performance. It is practical to use this in an actual ventilation ductwork system, and it has a potential application in noise control with longitudinal space limitation.

Acknowledgements

The work described in this paper was fully supported by a grant from the Research Grants Council of the Hong Kong Special Administrative Region, China (Project No. PolyU 152116/14E).

References

[1] Mak CM, Wu J, Ye C, Yang J. Flow noise from spoilers in ducts. J Acoust Soc Am 2009;125(6):3756-3765.

[2] Fry A. Noise Control in Building Services. Oxford: Pergamon; 1987.

[3] Mak CM, Wang Z. Recent advances in building acosutics: An overviwe of prediction methods and their applications. Build Environ 2015;91:118-126.

[4] Peat KS, Rathi KL. A finite element analysis of the convected acoustic wave motion in dissipative silencers. J Sound Vib 1995;184(3):529-545.

[5] Hansen CH, Snyder SD. Active Control of Noise and Vibration. London: E&FN Spon; 1997.

[6] Chen K, Paurobally R, Pan J, Q XJ. Improving acitive control of fan noise with automatic spectral reshaping for reference singnal. Appl Acoust 2015;87:142-152.

[7] Ingard U. On the theory and design of acoustic resonators. J Acoust Sco Am 1953;25: 1037-1061.

[8] Cai C, Mak CM, Shi X. An extended neck versus a spiral neck of the Helmholz resonator. Appl Acoust 2017;115:74-80.

[9] Seo SH, Kim YH. Silencer design by using array resonators for low-freqeuncy band noise reduction. J Acoust Soc Am 2005;118(4):2332-2338.

[10] Sugimoto A, Horioka T. Dispersion characteristics of sound waves in a tunnel with an array of Helmholtz resonators. J Acoust Soc Am 1995;97(3):1446-1459.

[11] Wang X, Mak C.M. Disorder in a periodic Helmholtz resonators array. Appl Acoust 2014;82:1-5.

[12] Chiu MC. Numerical assessment for a broadband and tuned noise using hybrid mufflers and a simulated annealing method. J Sound Vib 2013;332:2913-2940.

[13] Coulon JM, Atalla N, Derochers A.Optimization of concentric array resonators for wide band noise reduction. Appl Acoust 2016;113:109-115.

[14] Rayleigh JWS. The theory of Sound. New York: Dover, 1945.

[15] Munjal ML. Acoustics of Ducts and Muffers. New York: Wiley, 1987.

[16] Selamet A, Dickey NS. Theoretical, computational and experimental investigation of Helmholtz resonators with fixed volume: lumped versus distributed analysis. J Sound Vib 1995;187(2):358-367.

[17] Ji ZL, Sha JZ. Four-pole parameter of a duct with low Mach number flow. J Acoust Soc Am 1995;98(5):2848-2850.

[18] Bradley CE. Time harmonic acoustic Bloch wave propagation in periodic waveguides. Part I. Theory. J Acoust Soc Am 1994;96:1844-1953.

[19] Wang X, Mak C.M. Wave propagation in a duct with a periodic Helmholtz resonator array. J Acoust Soc Am 2012;131(2):1172-1182.

[20] Cai C, Mak CM. Noise control zone for a periodic ducted Helmholtz resonator system. J Acoust Soc Am 2016;140(6):EL471-EL477.

[21] Langley RS. Wave transmission through one-dimensional near periodic structures: optimum and random disorder. J Sound Vib 1995;188(5):717-743.

[22] Mace BR. Reciprocity, conservation of energy and some properties of reflection and transmission coefficients. J Sound Vib 1992;155:375-381.

Figure captions

Fig. 1 A single side-branch Helmholtz resonator.

Fig. 2 A side-branch Helmholtz resonators (a) side view (b) front view.

Fig. 3 Schematic diagram of a periodic ducted HR system.

Fig. 4 Schematic diagram of a modified ducted HR system.

Fig. 5 Comparison of the transmission loss with respect to the number of identical HRs mounted on the same cross-section.

Fig.6 Comparison of the analytical predictions and the FEM simulation with respect to different HRs mounted on a same cross-section (solid lines represents the theoretical predictions, and dotted crosses represent the FEM simulation results).

Fig. 7 The average transmission loss of the ducted HR system with different numbers of HR.

Fig.8 The average transmission loss of the periodic ducted HR system with different number of HRs (solid lines represents the theoretical predictions, and dotted crosses represent the FEM simulation results).

Fig. 9 Configuration of three modified ducted HR system cases: (a) 2143 model, (b) 2131 model, (c) 1121 model (the integer means the number of HR mounted on the same cross-section in consecutive duct segment respectively).

Fig. 10 Comparison of transmission loss with respect to different ducted HR systems.

Fig.11 The average transmission loss of different modified HR system (solid lines represents the theoretical predictions, and dotted crosses represent the FEM simulation results).